First-order analysis of a three-lens afocal zoom system

Mau-Shiun Yeh
Shin-Gwo Shiue
Mao-Hong Lu, MEMBER SPIE
National Chiao Tung University
Institute of Electro-Optical Engineering
1001 Ta Hsueh Road
Hsin Chu 30050, Taiwan
E-mail: mhlu@jenny.nctu.edu.tw

Abstract. A general analysis for the first-order design of a three-lens afocal zoom system with one lens fixed is presented. The reasonable solution areas in the focal length diagrams with positive or negative magnification are derived and shown graphically. The relation between the two separations of the three lenses in zooming is found to be a hyperbola. According to the different locations of hyperbola centers, four cases are analyzed. From the four hyperbolic graphs, we get five different types of zoom systems. For each zoom type, we find the maximum range of magnification and the position where the maximum or minimum system length occurs during zooming. The zoom loci for the first or second lens fixed are also discussed. [S0091-3286(97)02204-6]

Subject terms: zoom lenses; zoom design.

Paper 33076 received July 30, 1996; revised manuscript received Nov. 13, 1996; accepted for publication Nov. 14, 1996.

1 Introduction

A zoom system is generally considered to consist of three parts: the focusing, zooming and fixed parts. The focusing part is placed in front of the zooming part to adjust the object distance. The zooming part is literally used for zooming and the fixed rear part serves to control the focal length or magnification and reduce the aberrations of the whole system. Several of the published papers[1] concerning zoom have concentrated on the first-order zoom design. We also proposed a two-optical-component method for designing zoom system and a first-order analysis for the two-conjugate zoom system.[2,3]

An afocal zoom system is one in which the entrance and exit marginal rays are parallel to the optical axis. For a typical afocal zoom system, at least three lenses are needed with one lens fixed and the other lenses moving. The first lens is referred to as the focusing part and the others are the zooming part. Although different types of afocal zoom systems have been designed and widely used in many optical systems, such as telescopes, viewing finders, optical scanning systems, etc., few of the related publications[4–10] discuss their solution distribution. Chuang et al.[11] discussed the solution areas of a three-lens afocal zoom system according to the combinations of focal length values of the three lenses. They described the relation between magnification and either of the two separations of lenses in zooming.

In this paper, we use the graphoanalytical method[12] to solve the first-order layout of the three-lens afocal zoom system. The possible solution areas in the focal length diagram are shown graphically for positive and negative magnifications. We find the relation between the two separations of lenses in zooming, which can be described with a hyperbola. We obtain four hyperbolas corresponding to the different positions of hyperbola centers in the interlens separation coordinate system. From the four hyperbolic graphs, we can get five types of zoom systems and find the maximum range of magnification for each zoom type. The zoom position where the system has the maximum or minimum length is described. We discuss the zoom loci with the first or central lens fixed.

2 Theory

2.1 *Basic Formulas*

The afocal zoom system, consisting of three lenses with one lens fixed and the others moving, has been analyzed with the two-optical-component method,[2] in which the first lens is considered as one component and lenses 2 and 3 are combined as the second component. For an infinite-conjugate system, as shown in Fig. 1, the second focal point of lens 1 coincides with the first focal point of the combined unit. The related equations are then given by

$$D_1 = F_1 + F_{23} = d_1 + \delta, \tag{1}$$

$$\delta = \frac{F_{23}}{F_3} d_2, \tag{2}$$

$$K_{23} = K_2 + K_3 - K_2 K_3 d_2, \tag{3}$$

$$M = -\frac{F_1}{F_{23}} = \frac{h_1}{h_3}, \tag{4}$$

where K and F are the equivalent power and focal length of a lens, respectively. The combined component has the focal length F_{23} and power K_{23}; d_1 and d_2 are the separations between lenses 1 and 2 and between lenses 2 and 3, respectively; M is the magnification of system; δ is the distance

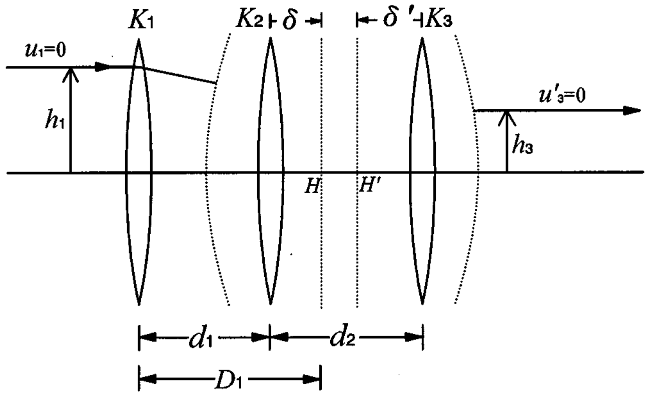

Fig. 1 Gaussian diagram of three-lens afocal zoom system: $\delta(\delta')$ is the distance from the first (second) lens to the first (second) principal plane $H(H')$ of the combined unit.

from the first lens to the first principal plane H of the combined unit of lenses 2 and 3; and h is the height of marginal ray at lens.

Solving the preceding equations, we have

$$d_1=F_1+F_2+\frac{F_1F_2}{F_3M}, \tag{5}$$

$$d_2=F_2+F_3+\frac{F_2F_3M}{F_1}. \tag{6}$$

In zooming, we change M and then obtain d_1 and d_2. The results are suitable for the case in which any one of the three lenses is fixed during zooming. Because the afocal system with the front lens fixed is the reverse case with the rear lens fixed, the analyses for these two cases are the same. Thus we discuss only the system with the first or second lens fixed in zooming.

2.2 *Solution Areas in the Focal Length Diagram*

Rewrite Eqs. (5) and (6) as

$$d_1=a_1+\frac{b_1}{M}, \tag{7}$$

$$d_2=a_2+b_2M, \tag{8}$$

where

$$a_1=F_1+F_2, \quad b_1=\frac{F_1F_2}{F_3}, \quad a_2=F_2+F_3,$$

and

$$b_2=\frac{F_2F_3}{F_1}.$$

The separations d_1 and d_2 must be positive in zooming. This provides some constraints on the solutions for a_1, a_2, b_1, b_2, and M in the focal length diagram. From Eq. (5), we have

$$F_1+F_2+\left(\frac{1}{F_3M}\right)F_1F_2\geqslant 0. \tag{9}$$

In the F_1 versus F_2 coordinate graph, the curve $F_1+F_2+F_1F_2/(F_3M)=0$ is a hyperbola with its center at $(-F_3M,-F_3M)$. The solution distribution in the graph is divided into several areas by the hyperbolic curves. Each solution area has different solution ranges for M and d_1.

Similarly, we have the following inequality equation from Eq. (6).

$$F_2+F_3+\left(\frac{M}{F_1}\right)F_2F_3\geqslant 0. \tag{10}$$

In the F_2 versus F_3 coordinate graph, the curve $F_2+F_3+(M/F_1)F_2F_3=0$ is also a hyperbola with its center at $(-F_1/M,-F_1/M)$. The solution distribution in the graph is also divided into several areas by the hyperbolic curves. Each solution area has different solution ranges for M and d_2.

From the preceding analysis, we can illustrate the possible solution areas in the focal length diagrams according to the different combinations of F_1, F_2, F_3 and the sign of M. Figs. 2 and 3 show the solution areas with positive M under the conditions of positive d_1 and d_2, respectively. The signs of three lens powers in each area are shown in parentheses as (F_1,F_2,F_3). The signs of $a_1(=F_1+F_2)$ in Fig. 2 and $a_2(=F_2+F_3)$ in Fig. 3 are positive in the upper-right section and negative in the lower-left section of coordinate graph. Similarly, Figs. 4 and 5 show the solution areas with negative M for positive d_1 and d_2, respectively.

2.3 *Relation Between M and the Interlens Separation d_1 or d_2*

The relation between M and one of the two interlens separations can be drawn with Eq. (5) or Eq. (6). Chuang et al.[11] described the results in their paper. The relations are hyperbolic between M and d_1 and linear between M and d_2.

2.4 *Relation Between the Two Interlens Separations d_1 and d_2*

From Eqs. (5) and (6), we have

$$[d_1-(F_1+F_2)][d_2-(F_2+F_3)]=F_2^2, \tag{11}$$

or

$$(d_1-a_1)(d_2-a_2)=F_2^2. \tag{12}$$

The preceding equation describes a hyperbola with its center at the coordinates (a_1,a_2) in the d_1 to d_2 coordinate graph. Because the center of hyperbola can be located in any quadrant, we obtain four cases of hyperbolas shown in

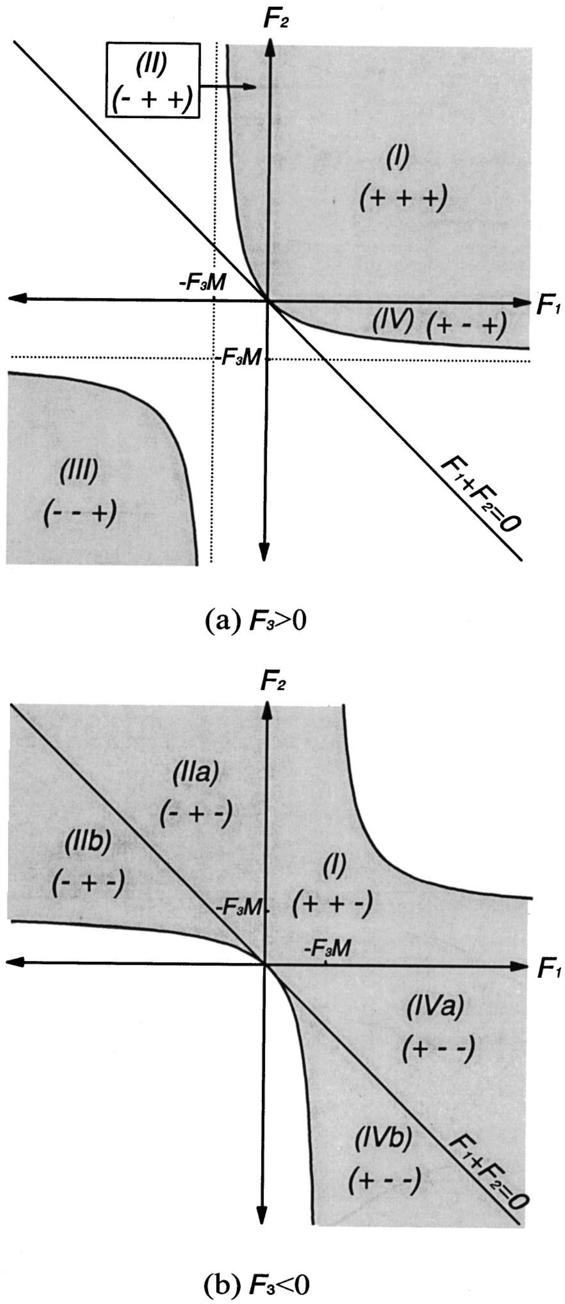

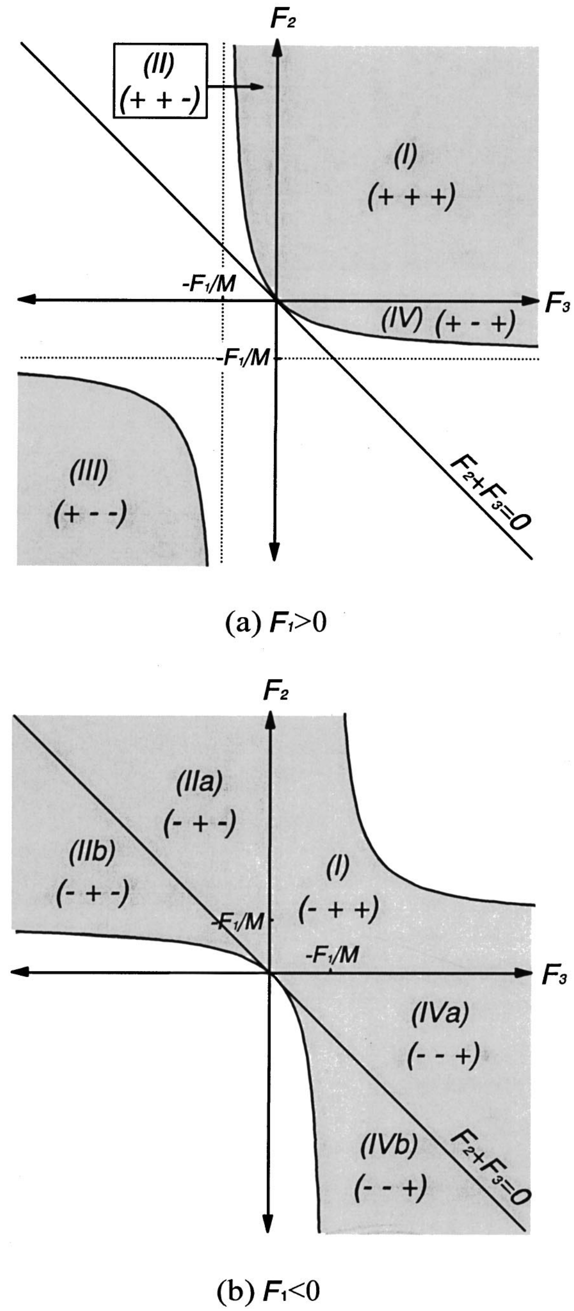

Fig. 2 Solution areas (shadowed) for different combinations of lens types with positive M, and (a) $F_3>0$ and (b) $F_3<0$ under the condition of positive d_1.

Fig. 3 Solution areas for different combinations of lens types with positive M, and (a) $F_1>0$ and (b) $F_1<0$ under the condition of positive d_2.

Figs. 6(a) to 6(d) depending on the signs of a_1 and a_2. From Eqs. (7) and (8), we can solve the magnification for each point on the hyperbola in Fig. 6, given by

$$M=\frac{b_1}{d_1-a_1}, \tag{13}$$

or

$$M=\frac{d_2-a_2}{b_2}. \tag{14}$$

In Eq. (13), if d_1 approaches the infinity, the magnification M approaches zero. If d_2 in Eq. (14) approaches the infinity, the magnification M approaches the infinity and the sign of M is determined by the sign of d_2/b_2. If $b_2(=F_2F_3/F_1)>0$, the magnifications for points on the upper-right hyperbolic curve are positive and on the lower-left hyperbolic curve are negative. On the other hand, if $b_2<0$, the magnifications for points on the upper-right and lower-left hyperbolic curves are negative and positive, respectively.

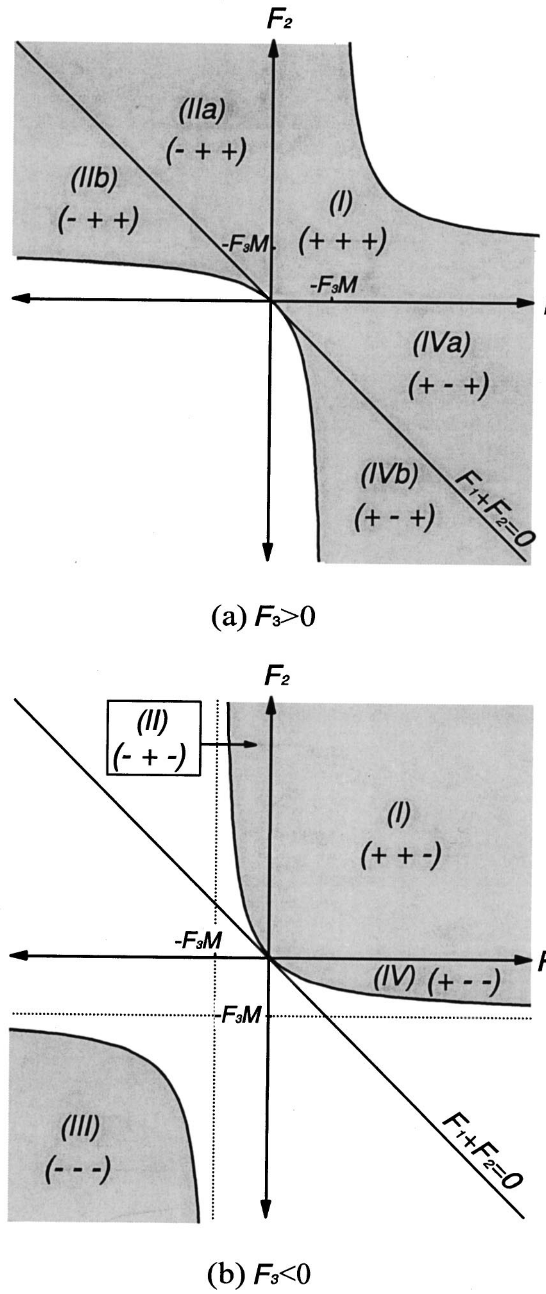

Fig. 4 Solution areas for different combinations of lens types with negative M, and (a) $F_3>0$ and (b) $F_3<0$ under the condition of positive d_1.

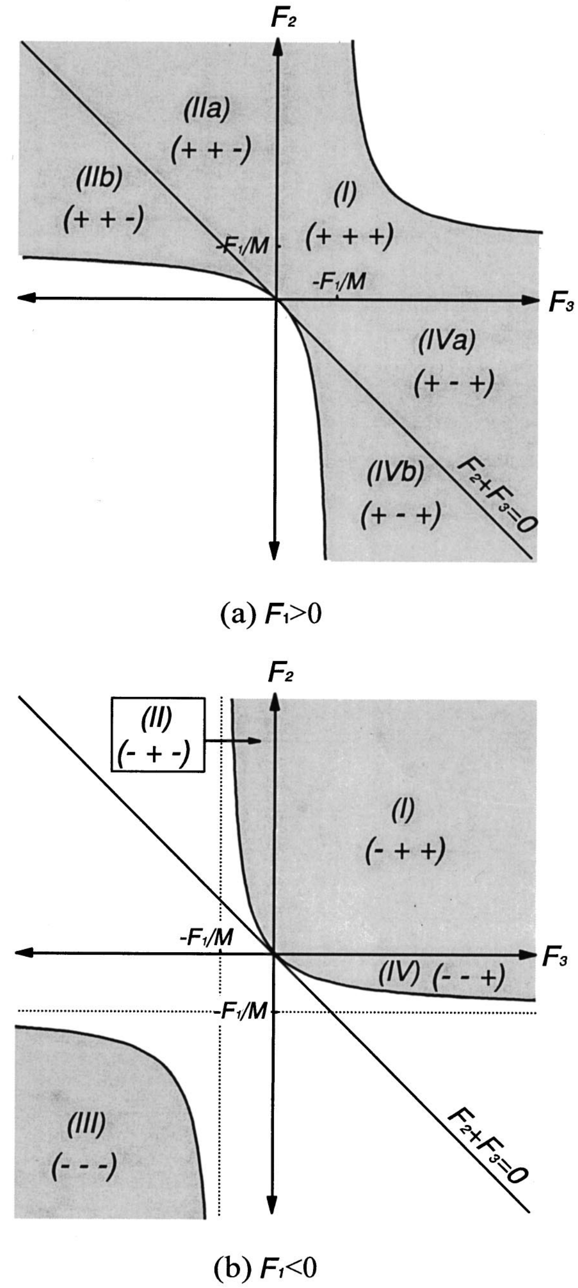

Fig. 5 Solution areas for different combinations of lens types with negative M, and (a) $F_1>0$ and (b) $F_1<0$ under the condition of positive d_2.

In Fig. 6, the intersections of hyperbola and the two axes are x and y corresponding to $d_2=0$ and $d_1=0$, respectively. From Eq. (14) with $d_2=0$, the magnification at point x is

$$M_x=-\frac{a_2}{b_2}. \tag{15}$$

Substituting Eq. (15) into Eq. (13) at point x, we have

$$d_1=a_1-\frac{b_1b_2}{a_2}. \tag{16}$$

Similarly, the magnification M_y and the value of d_2 at point y are obtained with $d_1=0$ in Eq. (13). We have

$$M_y=-\frac{b_1}{a_1}, \tag{17}$$

$$d_2=a_2-\frac{b_1b_2}{a_1}. \tag{18}$$

In fact, the separations d_1 and d_2 must be positive in zooming simultaneously. Thus only the segments of hyper-

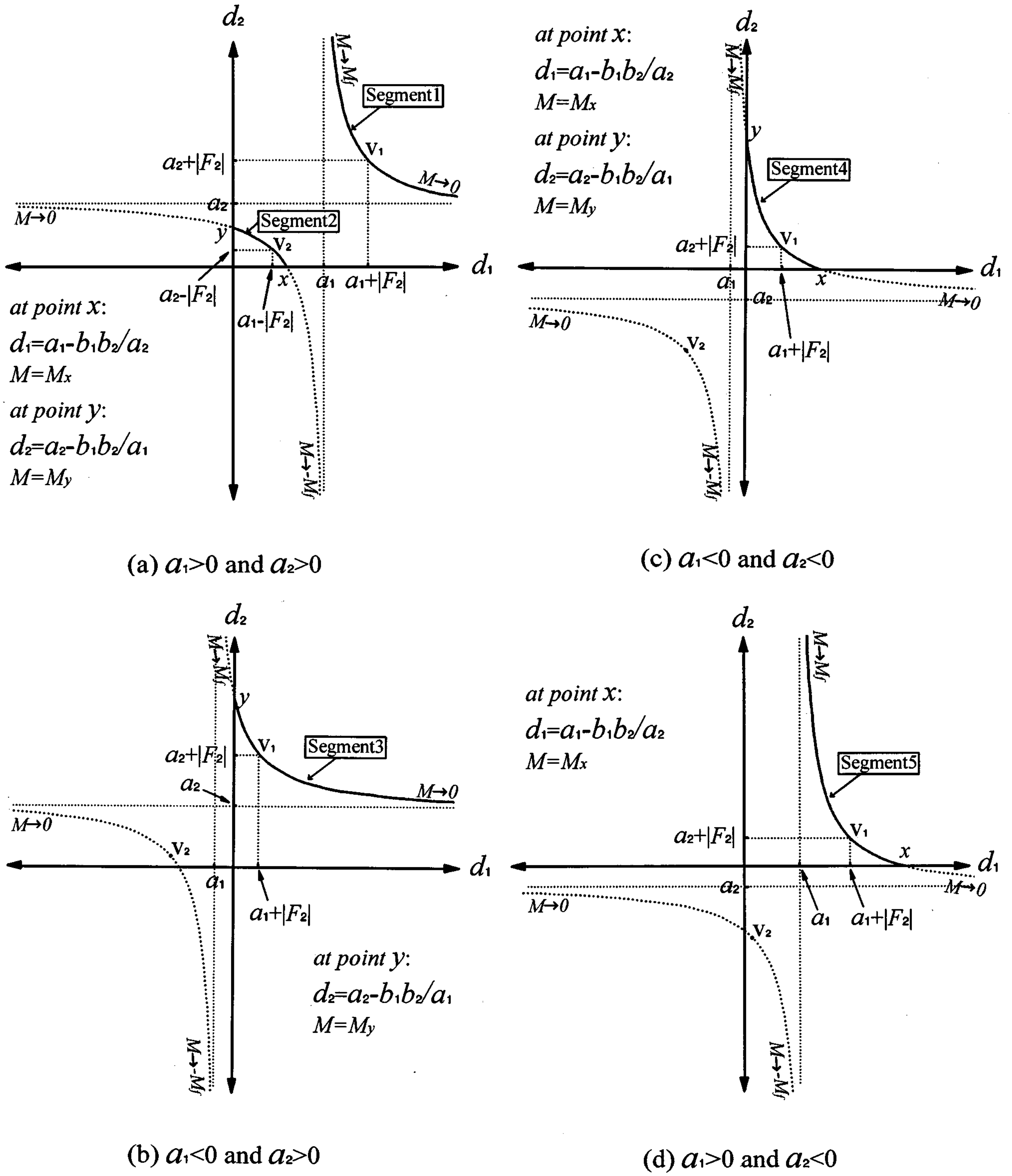

Fig. 6 Diagrams d_1 versus d_2 for the centers of hyperbolas located in the four quadrants, respectively; V_1 and V_2 are the vertexes of hyperbola. The magnification M_f is the plus infinity if $(F_2F_3/F_1)>0$ and the minus infinity if $(F_2F_3/F_1)<0$. The intersection coordinates of hyperbola and two axes are x and y, respectively.

bola in the first quadrant of the d_1 versus d_2 coordinate graph are acceptable and are shown with solid lines in Fig. 6. Five possible segments are found and marked by ''Segment'' followed by a number. Each segment represents the characteristics of a zoom system, including the constraints on a_1 and a_2 (i.e., on F_1, F_2, F_3) and the solution ranges of d_1, d_2, and M in zooming. Therefore, we can have five types of zoom systems.

From the property of hyperbola, the value of d_1+d_2 has the minimum at the vertex V_1 with $d_1=a_1+|F_2|$ and $d_2=a_2+|F_2|$ for segments 1, 3, 4, and 5 and has the maximum at the vertex V_2 with $d_1=a_1-|F_2|$ and $d_2=a_2-|F_2|$ for segment 2. Thus the system length, which is the distance from lens 1 to lens 3, has an extreme value (maximum or minimum) at some position of zooming, i.e., not necessarily at the one end of zooming, if the vertex of hyperbolic curve falls in the first quadrant. In this case, the magnification M is calculated as follows.

Substituting $d_1=a_1+|F_2|$ or $d_2=a_2+|F_2|$ into Eq. (13) or (14) for segments 1, 3, 4, and 5, we have

$$M=\frac{F_1}{F_3} \quad \text{if } F_2>0, \tag{19}$$

$$M=-\frac{F_1}{F_3} \quad \text{if } F_2<0. \tag{20}$$

Similarly, substituting $d_1=a_1-|F_2|$ or $d_2=a_2-|F_2|$ into Eq. (13) or (14) for segment 2, we have

$$M=-\frac{F_1}{F_3} \quad \text{if } F_2>0, \tag{21}$$

$$M=\frac{F_1}{F_3} \quad \text{if } F_2<0. \tag{22}$$

On the other hand, if the vertex of hyperbolic curve is outside the first quadrant, the maximum and minimum system lengths occur at the two ends of zooming.

For the lower-left hyperbolic curve in Fig. 6(a) or the upper-right hyperbolic curve in Fig. 6(c), the vertex can be located in any quadrant. If the vertex falls in the third quadrant, the whole hyperbolic curve is outside the first quadrant. Hence segment 2 or segment 4 disappears and no solution exits. If the vertex falls in the second or fourth quadrant, then the solution range of zooming is determined by the part that is in the first quadrant. So it is possible that no solution exits if the hyperbolic curve is outside the first quadrant.

2.5 *Common Solution Areas for Positive d_1 and d_2*

From Sec. 2.2 and Sec. 2.4, we find that the solution ranges of M and d_1 (or d_2) for each solution area in Figs. 2 and 4 (or Figs. 3 and 5) are always a part of hyperbola in Fig. 6, where d_1 (or d_2) is positive. So we can combine the solution areas in Figs. 2 and 3 to obtain 12 common solution areas with positive magnification M. Each of them represents an overlapped solution area where d_1 and d_2 are both positive. Similarly, we can obtain 11 common solution areas with negative magnification M from Figs. 4 and 5. The results are shown in Tables 1 and 2.

Tables 1 and 2 also show the constraints on the signs of a_1 and a_2, the used segment of hyperbola in the d_1 versus d_2 coordinate graph, and the possible vertex locations of related hyperbolic curve in the four quadrants for each common solution area. The various quadrants are denoted by I, II, III, and IV, respectively. The maximum ranges of M and the related ranges of d_1 and d_2 are also described.

For the third and sixth combinations in Table 1, segment 2 in Fig. 6(a) is used and the vertex of related hyperbolic curve is located in the fourth and second quadrants, respectively. In those two cases, we have $b_2<0$ (or $F_2F_3/F_1<0$), so the magnifications of points on the lower-left hyperbolic curve in Fig. 6(a) are positive. The solution exists only if segment 2 exists; in this case, $M_y \leqslant M_x$ is a necessary condition. Similar cases occur in the second, fifth, tenth and twelfth combinations in Table 1. For the tenth and eleventh combinations in Table 2, no solution exists because the vertex of related hyperbolic curve always falls in the third quadrant.

2.6 *Five Types of Zoom Systems*

As has been mentioned, each of the five segments in Fig. 6 represents the characteristics of a zoom system. Five different types of zoom systems are thus discussed as follows.

2.6.1 *Type I*

For segment 1 in Fig. 6(a), the range of system magnification can be from plus or minus infinity to zero depending on the sign of b_2. Because the vertex of related hyperbolic curve is located in the first quadrant, the system length always passes through a minimum value during zooming. In this case, we choose the second common solution area in Table 2 as an example. According to the constraints on F_1, F_2, and F_3 in the solution areas marked with (IVa) in Fig. 4(a) and (IVa) in Fig. 5(a), we give $F_1=1$, $F_2=-0.5$, and $F_3=1.1$. The maximum range of magnification can be from minus infinity to zero. Here we choose the range of M from -10 to -0.1 with a zoom ratio of 100:1. When the system length has the minimum value, we have $d_1=1.000$, $d_2=1.100$, and $M=-0.909$. The lens loci in zooming with the first lens fixed are shown in Fig. 7, with the natural logarithm of the magnification as ordinate. If the system with the second lens fixed is used, the zoom loci are as shown in Fig. 8.

2.6.2 *Type II*

For segment 2 in Fig. 6(a), the range of system magnification is from M_x to M_y. Here we choose the second common solution area in Table 1 as an example. Under the constraints on F_1, F_2, and F_3 in the solution areas marked with (IV) in Fig. 2(a) and (IV) in Fig. 3(a), we give $F_1=1$, $F_2=-0.3$, and $F_3=1.2$. So we have $M_x=2.500$ at $d_1=0.600$ and $d_2=0$, and $M_y=0.357$ at $d_1=0$ and $d_2=0.771$. The system has the maximum length with $d_1=0.400$, $d_2=0.600$, and $M=0.833$. The zoom loci with the first lens fixed are shown in Fig. 9. If the system with the central lens fixed is used, the lens loci in zooming are as shown in Fig. 10.

2.6.3 *Type III*

For segment 3 in Fig. 6(b), the range of system magnification is from M_y to 0. In this type, the vertex of hyperbolic curve can be located in the first or second quadrant. Here we use the ninth common solution area in Table 1 as an example. Referring to the solution areas marked with (IIb)

Table 1 Solutions for three-lens afocal zoom system with positive magnification.

Types of Lenses		Common Solution Areas for Positive d_1 and d_2		Used Segment and Possible Location of Vertex of Related Hyperbolic Curve		Solution Ranges of M, d_1, and d_2		
$F_1>0$, $F_2>0$, $F_3>0$ $(+++)$	1	(I), Fig. 2(a)	(I), Fig. 3(a)	Segment 1 ($a_1>0$, $a_2>0$)	Quad. I	$0<M<\infty$	$a_1<d_1<\infty$	$a_2<d_2<\infty$
$F_1>0$, $F_2<0$, $F_3>0$ $(+-+)$	2	(IV), Fig. 2(a)	(IV), Fig. 3(a)	Segment 2 ($a_1>0$, $a_2>0$)	Quad. I–IV	If $M_y\leqslant M_x$, then $M_y\leqslant M\leqslant M_x$	$0\leqslant d_1\leqslant a_1-\frac{b_1b_2}{a_2}$	$0\leqslant d_2\leqslant a_2-\frac{b_1b_2}{a_1}$
$F_1>0$, $F_2>0$, $F_3<0$ $(++-)$	3	(I), Fig. 2(b)	(II), Fig. 3(a)	Segment 2 ($a_1>0$, $a_2>0$)	Quad. IV	If $M_y\leqslant M_x$, then $M_y\leqslant M\leqslant M_x$	$0\leqslant d_1\leqslant a_1-\frac{b_1b_2}{a_2}$	$0\leqslant d_2\leqslant a_2-\frac{b_1b_2}{a_1}$
$F_1>0$, $F_2<0$, $F_3<0$ $(+--)$	4	(IVa), Fig. 2(b)	(III), Fig. 3(a)	Segment 5 ($a_1>0$, $a_2<0$)	Quad. IV	$M_x\leqslant M<\infty$	$a_1<d_1\leqslant a_1-\frac{b_1b_2}{a_2}$	$0\leqslant d_2<\infty$
	5	(IVb), Fig. 2(b)	(III), Fig. 3(a)	Segment 4 ($a_1<0$, $a_2<0$)	Quad. IV	If $M_x\leqslant M_y$, then $M_x\leqslant M\leqslant M_y$	$0\leqslant d_1\leqslant a_1-\frac{b_1b_2}{a_2}$	$0\leqslant d_2\leqslant a_2-\frac{b_1b_2}{a_1}$
$F_1<0$, $F_2>0$, $F_3>0$ $(-++)$	6	(II), Fig. 2(a)	(I), Fig. 3(b)	Segment 2 ($a_1>0$, $a_2>0$)	Quad. II	If $M_y\leqslant M_x$, then $M_y\leqslant M\leqslant M_x$	$0\leqslant d_1\leqslant a_1-\frac{b_1b_2}{a_2}$	$0\leqslant d_2\leqslant a_2-\frac{b_1b_2}{a_1}$
$F_1<0$, $F_2>0$, $F_3<0$ $(-+-)$	7	(IIa), Fig. 2(b)	(IIa), Fig. 3(b)	Segment 1 ($a_1>0$, $a_2>0$)	Quad. I	$0<M<\infty$	$a_1<d_1<\infty$	$a_2<d_2<\infty$
	8	(IIa), Fig. 2(b)	(IIb), Fig. 3(b)	Segment 5 ($a_1>0$, $a_2<0$)	Quad. I, IV	$M_x\leqslant M<\infty$	$a_1<d_1\leqslant a_1-\frac{b_1b_2}{a_2}$	$0\leqslant d_2<\infty$
	9	(IIb), Fig. 2(b)	(IIa), Fig. 3(b)	Segment 3 ($a_1<0$, $a_2>0$)	Quad. I, II	$0<M\leqslant M_y$	$0\leqslant d_1<\infty$	$a_2<d_2\leqslant a_2-\frac{b_1b_2}{a_1}$
	10	(IIb), Fig. 2(b)	(IIb), Fig. 3(b)	Segment 4 ($a_1<0$, $a_2<0$)	Quad. I–IV	If $M_x\leqslant M_y$, then $M_x\leqslant M\leqslant M_y$	$0\leqslant d_1\leqslant a_1-\frac{b_1b_2}{a_2}$	$0\leqslant d_2\leqslant a_2-\frac{b_1b_2}{a_1}$
$F_1<0$, $F_2<0$, $F_3>0$ $(--+)$	11	(III), Fig. 2(a)	(IVa), Fig. 3(b)	Segment 3 ($a_1<0$, $a_2>0$)	Quad. II	$0<M\leqslant M_y$	$0\leqslant d_1<\infty$	$a_2<d_2\leqslant a_2-\frac{b_1b_2}{a_1}$
	12	(III), Fig. 2(a)	(IVb), Fig. 3(b)	Segment 4 ($a_1<0$, $a_2<0$)	Quad. II	If $M_x\leqslant M_y$, then $M_x\leqslant M\leqslant M_y$	$0\leqslant d_1\leqslant a_1-\frac{b_1b_2}{a_2}$	$0\leqslant d_2\leqslant a_2-\frac{b_1b_2}{a_1}$

Table 2 Solutions for three-lens afocal zoom system with negative magnification.

Types of Lenses		Common Solution Areas for Positive d_1 *and* d_2		Used Segment and Possible Location of Vertex of Related Hyperbolic Curve		Solution Ranges of M, d_1, *and* d_2		
$F_1>0$, $F_2>0$, $F_3>0$ $(+++)$	1	(I), Fig. 4(a)	(I), Fig. 5(a)	Segment 2 ($a_1>0$, $a_2>0$)	Quad. I	$M_x\leqslant M\leqslant M_y$	$0\leqslant d_1\leqslant a_1-\frac{b_1b_2}{a_2}$	$0\leqslant d_2\leqslant a_2-\frac{b_1b_2}{a_1}$
$F_1>0$, $F_2<0$, $F_3>0$ $(+-+)$	2	(IVa), Fig. 4(a)	(IVa), Fig. 5(a)	Segment 1 ($a_1>0$, $a_2>0$)	Quad. I	$-\infty<M<0$	$a_1<d_1<\infty$	$a_2<d_2<\infty$
	3	(IVa), Fig. 4(a)	(IVb), Fig. 5(a)	Segment 5 ($a_1>0$, $a_2<0$)	Quad. I	$-\infty<M\leqslant M_x$	$a_1<d_1\leqslant a_1-\frac{b_1b_2}{a_2}$	$0\leqslant d_2<\infty$
	4	(IVb), Fig. 4(a)	(IVa), Fig. 5(a)	Segment 3 ($a_1<0$, $a_2>0$)	Quad. I	$M_y\leqslant M<0$	$0\leqslant d_1<\infty$	$a_2<d_2\leqslant a_2-\frac{b_1b_2}{a_1}$
	5	(IVb), Fig. 4(a)	(IVb), Fig. 5(a)	Segment 4 ($a_1<0$, $a_2<0$)	Quad. I	$M_y\leqslant M\leqslant M_x$	$0\leqslant d_1\leqslant a_1-\frac{b_1b_2}{a_2}$	$0\leqslant d_2\leqslant a_2-\frac{b_1b_2}{a_1}$
$F_1>0$, $F_2>0$, $F_3<0$ $(++-)$	6	(I), Fig. 4(b)	(IIa), Fig. 5(a)	Segment 1 ($a_1>0$, $a_2>0$)	Quad. I	$-\infty<M<0$	$a_1<d_1<\infty$	$a_2<d_2<\infty$
	7	(I), Fig. 4(b)	(IIb), Fig. 5(a)	Segment 5 ($a_1>0$, $a_2<0$)	Quad. I, IV	$-\infty<M\leqslant M_x$	$a_1<d_1\leqslant a_1-\frac{b_1b_2}{a_2}$	$0\leqslant d_2<\infty$
$F_1<0$, $F_2>0$, $F_3>0$ $(-++)$	8	(IIa), Fig. 4(a)	(I), Fig. 5(b)	Segment 1 ($a_1>0$, $a_2>0$)	Quad. I	$-\infty<M<0$	$a_1<d_1<\infty$	$a_2<d_2<\infty$
	9	(IIb), Fig. 4(a)	(I), Fig. 5(b)	Segment 3 ($a_1<0$, $a_2>0$)	Quad. I, II	$M_y\leqslant M<0$	$0\leqslant d_1<\infty$	$a_2<d_2\leqslant a_2-\frac{b_1b_2}{a_1}$
$F_1<0$, $F_2>0$, $F_3<0$ $(-+-)$	10	(II), Fig. 4(b)	(II), Fig. 5(b)	Segment 2 ($a_1>0$, $a_2>0$)	Quad. III	No solution	No solution	No solution
$F_1<0$, $F_2<0$, $F_3<0$ $(---)$	11	(III), Fig. 4(b)	(III), Fig. 5(b)	Segment 4 ($a_1<0$, $a_2<0$)	Quad. III	No solution	No solution	No solution

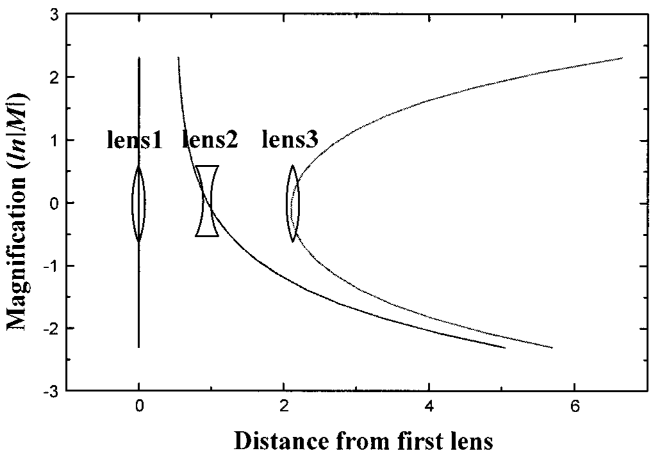

Fig. 7 Loci of three-lens afocal zoom system with $F_1=1$, $F_2=-0.5$, $F_3=1.1$, and zoom ratio=100. This system has $d_1=1.000$, $d_2=1.100$, and $M=-0.909$ at the position where the system length is minimum.

in Fig. 2(b) and (IIa) in Fig. 3(b), we give $F_1=-1$, $F_2=0.79$, and $F_3=-0.75$. We then have $M_y=5.016$ at $d_1=0$ and $d_2=3.012$. In example, we choose M from 5.016 to 0.200. The system has the minimum length with $d_1=0.580$, $d_2=0.830$, and $M=1.333$. The zoom loci with the first lens fixed are shown in Fig. 11.

2.6.4 *Type IV*

For segment 4 in Fig. 6(c), the range of system magnification is from M_y to M_x. Here we use the tenth common solution area in Table 1 as an example. According to the solution areas marked with (IIb) in Fig. 2(b) and (IIb) in Fig. 3(b), we give $F_1=-1$, $F_2=0.75$, and $F_3=-1$. So we have $M_x=0.333$ at $d_1=2.000$ and $d_2=0$, and $M_y=3.000$ at $d_1=0$ and $d_2=2.000$. The system has the minimum length with $d_1=0.500$, $d_2=0.500$, and $M=1.0$. The zoom loci with the first lens fixed are shown in Fig. 12.

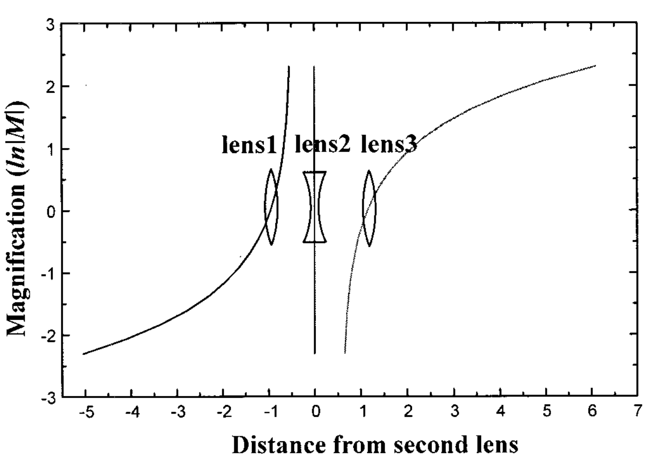

Fig. 8 Loci of three-lens afocal zoom system with the second lens fixed. The system parameters are the same as in Fig. 7.

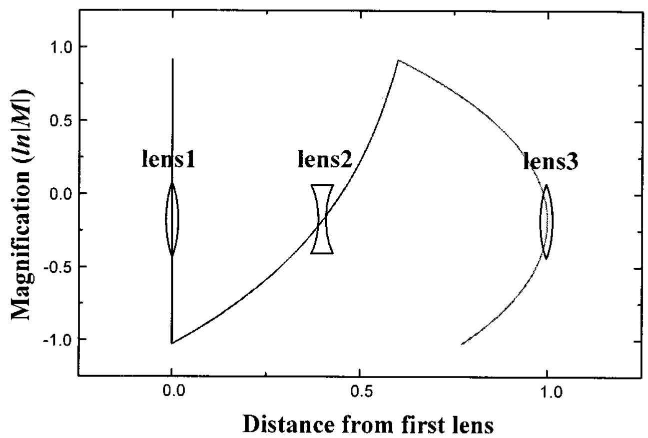

Fig. 9 Loci of three-lens afocal zoom system with $F_1=1$, $F_2=-0.3$, $F_3=1.2$, and zoom ratio=7. This system has $d_1=0.400$, $d_2=0.600$, and $M=0.833$ at the position where the system length is maximum.

2.6.5 *Type V*

For segment 5 in Fig. 6(d), the range of system magnification is from plus or minus infinity to M_x depending on the sign of b_2. In this type, the vertex of hyperbolic curve can be located in the first or fourth quadrant. We choose the third common solution area in Table 2 as an example. Referring to the solution areas marked with (IVa) in Fig. 4(a) and (IVb) in Fig. 5(a), we give $F_1=1$, $F_2=-0.66$, and $F_3=0.52$. We then have $M_x=-0.408$ at $d_1=3.451$ and $d_2=0$. In example, we choose the range of M from -10.200 to -0.408 with a zoom ratio of 25:1. When the system has the minimum length during zooming, we get $d_1=1.000$, $d_2=0.520$, and $M=-1.923$. The zoom loci with the first lens fixed are shown in Fig. 13.

3 Discussion

In this analysis, the graphoanalytical method[12] was used because of its convenience to show the connection between the solution space and the variable space used by the lens designer. For designing a zoom system, the size of system and the slope of lens loci are taken into account. In types I

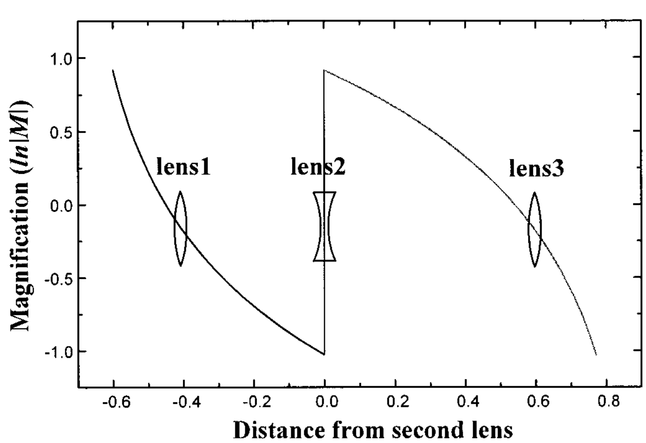

Fig. 10 Loci of three-lens afocal zoom system with the second lens fixed. The system parameters are the same as in Fig. 9.

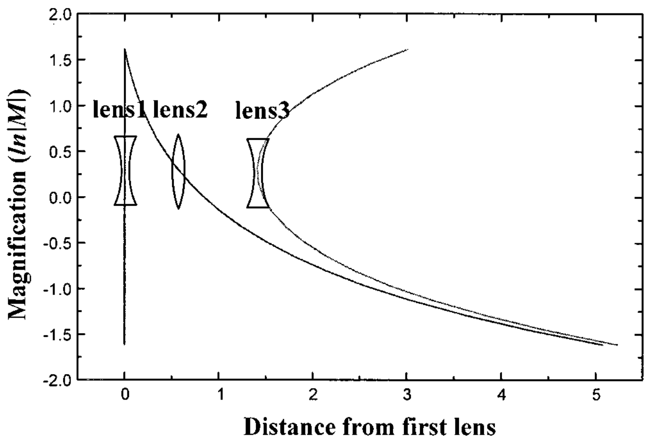

Fig. 11 Loci of three-lens afocal zoom system with $F_1=-1$, $F_2=0.79$, $F_3=-0.75$, and zoom ratio=25. This system has $d_1=0.580$, $d_2=0.830$, and $M=1.333$ at the position where the system length is minimum.

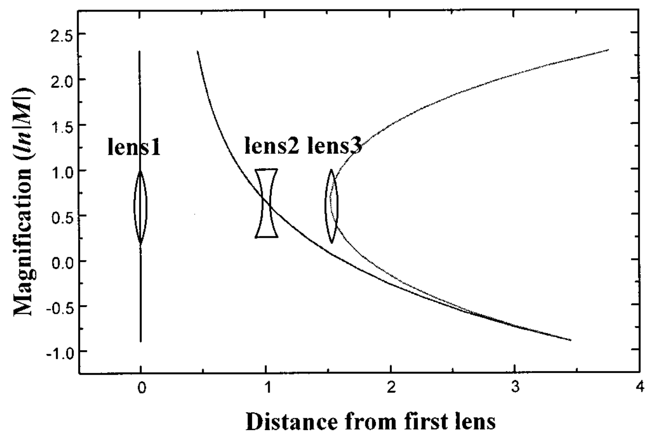

Fig. 13 Loci of three-lens afocal zoom system with $F_1=1$, $F_2=-0.66$, $F_3=0.52$, and zoom ratio=25. This system has $d_1=1.000$, $d_2=0.520$, and $M=-1.923$ at the position where the system length is minimum.

and II, two different results for the zoom loci with the first or second lens fixed are shown. Comparing Fig. 7 with Fig. 8 or comparing Fig. 9 with Fig. 10, we find that the system with the first lens fixed is more compact than that with the second lens fixed. This result is also true for types III to V since the relation between the two interlens separations is similar to that in type I. From the five types of systems, we find that only type II has the result that the maximum system length occurs inside the process of zooming. In some examples, we have the interlens separation equal to zero at one end of zooming. Usually, it is not useful to work in the neighborhood of the end in practical design. Note that we use the natural logarithm of the magnification as ordinate in Figs. 7 to 13. If the second lens is fixed during zooming, the third lens moves linearly according to Eq. (6). In this paper, we have not discussed the special condition in which $a_1=0$ $(F_1+F_2=0)$ or $a_2=0$ $(F_2+F_3=0)$ or both. The solution is easily obtained by the same way as described in Sec. 2. In this case, the center of hyperbola in Eq. (12) is located on the axis in the d_1 versus d_2 coordinate graph.

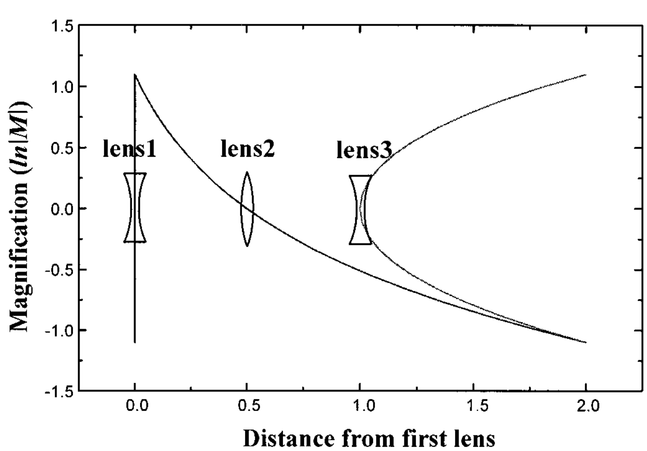

Fig. 12 Loci of three-lens afocal zoom system with $F_1=-1$, $F_2=0.75$, $F_3=-1$, and zoom ratio=9. This system has $d_1=0.500$, $d_2=0.500$, and $M=1.0$ at the position where the system length is minimum.

4 Conclusion

As we know, a proper first-order layout will often give a satisfactory lens design. For the first-order design of three-lens afocal zoom system, we have analyzed the possible solutions areas in the focal length diagram, the relation between M, d_1, and d_2, and the properties of lens loci during zooming. The common solution areas for positive d_1 and d_2 and their solution ranges of system parameters with positive or negative magnification have been presented. The analysis of five system types, corresponding to five segments in the d_1 versus d_2 coordinate graph, is helpful for designers to select the positive and negative types of three lenses, preview the shape of lens loci, and determine the ranges of M, d_1, and d_2.

Acknowledgments

This project was supported by the National Science Council of the Republic of China under the grant No. NSC-85-2215-E-009-004.

References

1. Allen Mann, Ed., *Selected Papers on Zoom Lenses*, SPIE Milestone Series, Vol. MS 85, SPIE Press, Bellingham, WA (1993).
2. M. S. Yeh, S. G. Shiue, and M. H. Lu, ''Two-optical-component method for designing zoom system,'' *Opt. Eng.* **34**(6), 1826–1834 (1995).
3. M. S. Yeh, S. G. Shiue, and M. H. Lu, ''First-order analysis of a two-conjugate zoom system,'' *Opt. Eng.* **35**(11), 3348–3360 (1996).
4. A. Mann, ''Infrared zoom lens system for target detection,'' *Opt. Eng.* **21**(4), 786–793 (1982).
5. M. Roberts, ''Compact infrared continuous zoom telescope,'' *Opt. Eng.* **23**(2), 117–121 (1984).
6. I. A. Neil, ''General purpose zoom lenses for the thermal infrared,'' *Proc. SPIE* **518**, 55–56 (1984).
7. M. Shechterman, ''High performance wide magnification range IR zoom telescope with automatic compensation for temperature effects,'' *Proc. SPIE* **1442**, 276–285 (1990).
8. R. Chen, X. Zhou, and X. Zhang, ''Design of compact IR zoom telescope,'' *Proc. SPIE* **1540**, 717–723 (1991).
9. R. E. Fischer and T. U. Kampe, ''Actively controlled 5:1 afocal zoom

attachment for common module FLIR,'' *Proc. SPIE* **1690**, 137–152 (1992).
10. R. B. Johnson and Chen Feng, ''Mechanically compensated zoom lenses with a single moving element,'' *Appl. Opt.* **31**(13), 2274–2278 (1992).
11. F. M. Chuang, M. W. Chang, and S. G. Shiue, ''Solution areas of three-component afocal zoom system,'' *Optik* **101**(1), 10–16 (1995).
12. M. L. Oskotsky, ''Grapho-analytical method for the first-order design of two-component zoom systems,'' *Opt. Eng.* **31**(5), 1093–1097 (1992).

Mau-Shiun Yeh received his BS from the National Taiwan Normal University and his MS from the National Central University. In 1997, he received his PhD in electro-optical engineering from National Chiao-Tung University. He is currently an associate researcher in optical lens design and metrology at the Chung Shan Institute of Science and Technology.

Shin-Gwo Shiue received his BS and MS degrees from the Chung-Cheng Institute of Technology, Taiwan, in 1973 and 1976, and a PhD degree from the University of Reading, United Kingdom, in 1984. He became an assistant researcher at the Chung Shan Institute of Science and Technology in 1976. Before receiving his PhD degree, his research interest was mainly solid state laser physics and afterward he concentrated in optical instrument design. He was a president of Taiwan Electro-Optical System company in 1990 and joined the Precision Instrument Developing Center of the National Science Council as a senior researcher in 1994. His current research is optical instrument developing, optical metrology, and lens design.

Mao-Hong Lu graduated from the Department of Physics at Fudan University in 1962. He was a research staff member at the Shanghai Institute of Physics and Technology, Chinese Academy of Sciences, from 1962 to 1970 and at Shanghai Institute of Laser Technology from 1970 to 1980. He studied at the University of Arizona as a visiting scholar from 1980 to 1982. He is currently a professor and director at the Institute of Electro-Optical Engineering, National Chiao-Tung University.